

The Computation of Radial Distribution Functions for Glassy Materials

BY J. H. KONNERT AND J. KARLE

Laboratory for the Structure of Matter, Naval Research Laboratory, Washington, D.C. 20375, U.S.A.

(Received 10 April 1973; accepted 22 June 1973)

A procedure is described for optimizing the extraction of information from the diffraction data of a glass. A least-squares technique that minimizes the spurious detail in the radial distribution function (RDF) at small and large interatomic distances is employed both to isolate that portion of the total intensity function which contains the interatomic distance information and to remove from this function contributions from the shortest distances, thus eliminating the major source of termination errors. X-ray diffraction data for silica glass is utilized to illustrate the procedure. It is apparent that the procedure would be also applicable to the liquid state.

Introduction

The determination of structural information for a glass is facilitated by an analysis of the distribution of interatomic distances. The distribution is expressed as a radial distribution function (RDF) which is computed from experimental scattering data. In utilizing RDF's for making interpretations, it is important to minimize the uncertainties in these functions, particularly for the larger interatomic distances. Such uncertainties are generated both by the data collection and the data reduction procedures.

Major improvements in data-reduction procedures are effected by the introduction of physical and mathematical criteria which must be satisfied by the distribution of distances. For example, the RDF should indicate zero probability for distances smaller than the shortest bonded distance, and, at sufficiently large distances, the RDF should indicate that all distances are equally probable. The imposition of constraints on RDF's has a long history and may be found in early studies of molecular structure by electron diffraction of gases (Karle & Karle, 1949, 1950).

A number of authors have developed procedures for introducing physical and mathematical criteria into the analytical procedures applied to diffraction data from glasses (Kaplow, Strong & Averbach, 1965; Warren, 1969; Leadbetter & Wright, 1972) with the objective of enhancing the reliability of the resulting RDF's. The procedure to be described here, while concerned with the same criteria, permits very rapid convergence of the data reduction by expressing the RDF explicitly as a function of refinable parameters defining the background intensity and short distances and employs a special method for treating the termination errors. Refinement of these parameters, subject to the aforementioned constraints, produces an RDF free from the errors associated with incorrect scaling of the data, incorrect background intensity, and termination of the data. Applications of the new technique have been made in recent investigations of silica and germania

glasses (Konnert & Karle, 1972; Konnert, Karle & Ferguson, 1973). The RDF's of these glasses were found to be consistent with a structure composed nearly entirely of ordered regions similar to tridymite, a crystalline polymorph of silica, having dimensions up to a least 20 Å and bonded efficiently together in configurations analogous to twinned crystals. In such a model the ordered regions have the same bonding topology as the crystalline polymorph and are distorted slightly owing to the junctions between the ordered regions. However, microcrystalline grain boundaries are not implied. The junctions may not vary significantly in energy and density from that in the ordered regions. Illustrative examples will be drawn from the data reduction of the X-ray diffraction data for silica glass.

The general theory relating the RDF to the diffraction pattern will be reviewed briefly at first, in order to facilitate the subsequent discussion. Sources of error in the RDF will then be discussed, followed by a description of the data reduction procedures used to minimize spurious details.

General theory

The total diffracted intensity from a glass, I_t , corrected for systematic effects such as scattering polarization and absorption, is comprised of the interatomic interference scattering, I , the coherent atomic scattering, I_c , and the incoherent atomic scattering, I_i . The pertinent equations are

$$I_t(s) = I(s) + I_c(s) + I_i(s) \quad (1)$$

$$= I(s) + I_b(s)$$

$$i(s) = [I_t(s) - I_b(s)] / \sum f^2(s) \quad (2)$$

where $s = 4\pi \sin \theta / \lambda$, 2θ is the angle between the incident and the diffracted beam, and λ is the wavelength. The sum of the squares of the coherent atomic scattering factors for the unit of composition, uc, e.g. SiO₂, is represented by $\sum f^2$. Division of I by $\sum f^2$ produces an intensity function, $i(s)$, that corresponds approximately

to the scattering intensity from vibrating point atoms.

A Fourier sine transform of $si(s)$ produces the radial distribution function $rD(r)$.

$$r^2D(r) = 4\pi r^2[\varrho(r) - \varrho_0] = \frac{2r}{\pi} \int_0^\infty si(s) \sin sr ds \quad (3)$$

where $4\pi r^2\varrho(r)$ represents the probability, weighted by the product of the scattering factors of atoms i and j divided by $\sum f^2$, of finding atoms j in the sample separated by the distance interval $(r, r + dr)$ from the atoms i . As will be seen, this relationship holds precisely only when $f_i f_j / \sum f^2$ does not vary with scattering angle. The bulk density parameter is ϱ_0 . The data reduction procedure isolates $i(s)$ from I_r , and Fourier analysis of $i(s)$ yields $D(r)$.

With the assumption of harmonic motion between pairs of atoms, the Fourier sine transform of $si(s)$ may be represented in terms of the interatomic distances and the bulk density,

$$r^2D(r) = \frac{2r}{\pi} \sum_{i,j} \frac{N_{ij}}{r_{ij}} \int_0^\infty \frac{f_i f_j}{\sum f^2} \times \exp(-l_{ij}^2 s^2 / 2) \sin sr_{ij} \sin sr ds \quad (4)$$

$$- 4\pi r^2 \varrho_0' \frac{(\sum_{uc} f_{(s=0)})^2}{\sum_{uc} f_{(s=0)}^2}$$

where r_{ij} is the distance between the i th and j th atoms, N_{ij} is the coordination number, l_{ij} is the disorder parameter, uc is the unit of composition, (SiO_2) and ϱ_0' is the bulk density in units of composition per \AA^3 . If there is no other source of disorder, l_{ij} is the root-mean-square amplitude of vibration. The first term on the right-hand side of equation (4) represents $4\pi r^2\varrho(r)$,

and the second term represents $4\pi r^2\varrho_0$. This second term is present in the Fourier sine transform of $si(s)$ since the extremely low-angle scattering, where all atoms in the sample are scattering in phase, is not contained in the experimentally measured $i(s)$. If the $f_i f_j / \sum f^2$ are not a function of s , the integral in equation (4) may be evaluated.

$$4\pi r^2\varrho(r) = \frac{2r}{\pi} \sum_{ij} \frac{N_{ij}}{r_{ij}} \frac{f_i f_j}{\sum f^2} \times \left[\exp\left(-\frac{(r_{ij}-r)^2}{2l_{ij}^2}\right) - \exp\left(-\frac{(r_{ij}+r)^2}{2l_{ij}^2}\right) \right] \quad (5)$$

The second exponential in the brackets is negligible for the values of r_{ij} present in glasses. Readers wishing more details on the general theory may refer to the early work in the field (Debye, 1915; Zernicke & Prins, 1927) or a textbook (Guinier, 1956; Warren, 1969).

Sources of error in RDF

The most troublesome errors aside from systematic ones, causing spurious detail in the RDF, are random errors in the experimental data, the limited scattering angle over which diffraction data may be collected, and the inaccurate separation of the interatomic scattering component from the total intensity. The limited scattering angle results in termination errors from the calculation of the integral in equation (3). In addition, the scattering factors for X-rays do not all have the same shape; *i.e.*, they do not differ from one another by only a scale factor. Therefore $f_i f_j / \sum f^2$ will vary somewhat as a function of s . Certain systematic errors may be present in experimental data owing to, for example, inadequate source collimation, extraneous instrumental background and incorrect absorption correction.

Data collection

The X-ray diffraction data for silica glass were collected in the range $0.3 \leq s \leq 16.0$ in intervals of 0.05 s with Mo $K\alpha$ radiation filtered with Zr so that the intensity ratio for $K\beta/K\alpha$ was 0.006. The cylindrical samples were 0.6–1.0 mm in diameter and the divergence of the beam was such that the intensity profile had a half-width at half-height of 0.08 s units at all scattering angles. Absorption corrections were made.

A pulse-height analyzer with window settings of 11.10 and 23.79 keV was also employed to eliminate spurious signals. The values for the data points at $s < 0.3$ were obtained by extrapolation to zero intensity at $s = 0$. The extrapolation is not arbitrary, but rather is subject to constraints imposed on the analysis.

The statistical accuracy of the data was monitored in order that the contribution of the random errors to the RDF could be assessed and reduced to the desired level. As equation (3) illustrates, an error of $\varepsilon(s)$ in $si(s)$

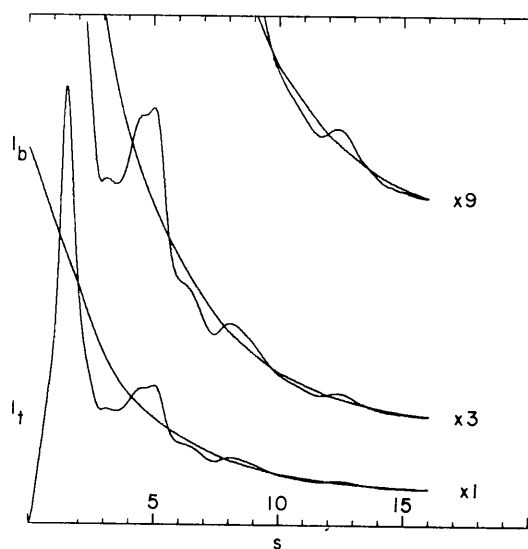


Fig. 1. The total X-ray diffraction pattern for silica glass, I_r , corrected for absorption and polarization, and the final representation for the background intensity, I_b .

extended to the region involving the distances that are removed.

2. The outer region of the RDF should show a uniform distribution of distances. In this context, termina-

tion effects and errors in the experimental data cause the outer region to have the appearance of a nonuniform distribution of distances and require correctional procedures.

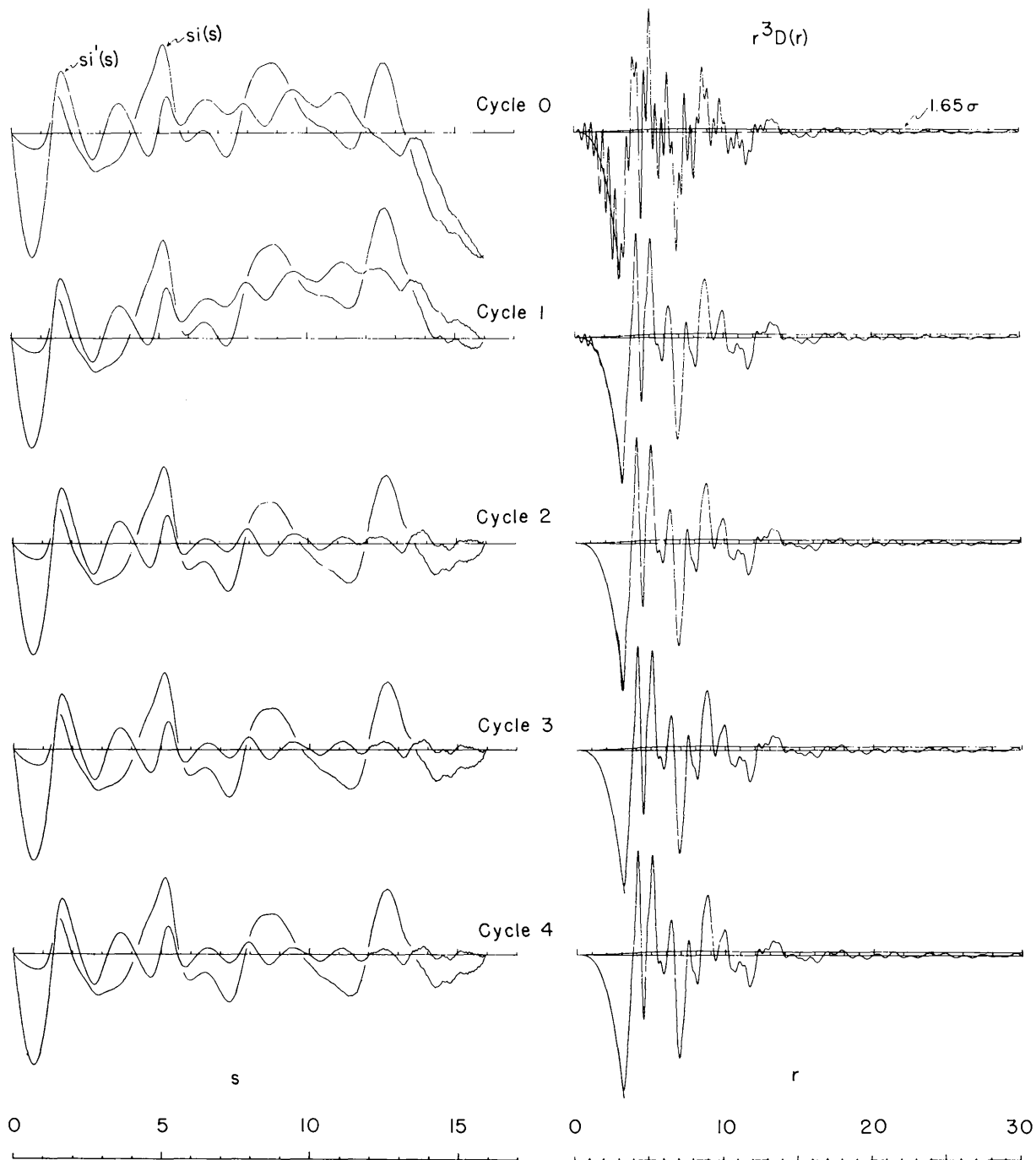


Fig. 2. The sharpened intensity functions $si(s)$, the corresponding functions minus the short distance contributions, $si'(s)$, and the RDF associated with $si'(s)$ for each cycle of the refinement. There is a 10% chance that the absolute value of an error in the RDF from random errors in the data will exceed the 1.65σ curve. The smooth curve accompanying $r^3D(r)$ at small r represents $-4\pi r^3 \rho_0$. The quantity r^3 is employed in order to scale the outer region with respect to the inner region of the RDF in a fashion which readily displays the features.

3. The scaling of the intensity data (and, thus, the RDF) should be consistent with the bulk-density measurement, known coordination number s or both.

4. The background scattering, I_b , should be a smoothly changing function whose shape is compatible with that expected from theory.

B. Initial representation of background intensity

The initial step in the data reduction procedure is to fit with exponential functions an approximate background intensity, I_b , obtained for example, from theoretical values for the scattering factors (Cromer & Mann, 1968) scaled to the total-intensity data. Use is made of overlapping functions of the form $\exp(a + bs^c)$ to represent I_b ,

$$I_b(s) = \sum_n W_n(s) \exp(a_n + b_n s^{c_n}) + d \cdot s, \quad (9)$$

a technique developed in the field of electron diffraction of gases (D'Antonio, George, Lowrey & Karle, 1971). Each exponential function overlaps to the midpoint of the adjacent exponential function and is assigned a weight, W_n , that varies linearly in the region of overlap from one at its midpoint to zero at the midpoint of the function with which it overlaps, with the exception of the terminal functions which have a weight of unity from their midpoints to the limits of the data. In the analysis of X-ray diffraction data d is set equal to zero. In treating neutron diffraction data, d is set to a non-zero value such that I_b is amenable to fitting with the exponential functions. The background intensity, as composed of its components, is smooth and sufficiently featureless so as not to affect the real distance contributions. This is accomplished by utilizing a limited number of exponential functions, especially in the initial stages of refinement, such that each function spans about 4–6 s units. This choice is particularly relevant to the shortest interatomic distance in the sample being studied. For silica the shortest distances are at approximately $\pi/2 A$. Reference to equation (4), which is discussed later, demonstrates that the intensity contribution for this distance is a sine function with a periodicity of about 4 s units. It is important to avoid the possibility of introducing an incorrect background function having an error with this periodicity or less.

C. Representation of RDF as a function of parameters defining I_b and short distances

The treatment of the termination error is based on the recognition that generally only the two or three shortest distances make a significant contribution to the experimental intensity function, $i(s)$, beyond the measured range of scattering angle, owing to their low thermal or disorder factors. The intensity functions corresponding to the larger distances are essentially damped out at the upper limit of the experimental data range, s_{\max} . The contributions from the shortest distances may be removed from $i(s)$ so that s_{\max} can ac-

curately replace infinity as the upper limit of the integral (3). Such an intensity function may also be written as a function of parameters defining I_b . The Fourier transform of such an intensity function, $i'(s)$, may be expressed by

$$r^2 D'(r) = 4\pi r^2 [\varrho'(r) - \varrho_0] \\ = \frac{2r}{\pi} \int_0^{s_{\max}} s i'(s) \exp(-\alpha s^2) \sin sr ds \quad (10)$$

$$i'(s) = i(s) - \sum_{sd} N_{ij} f_i f_j \exp(-l_{ij}^2 s^2 / 2) \\ \times \sin sr_{ij} / (sr_{ij} \sum f^2) \quad (11)$$

$$i(s) = \{I(s) - A [\sum_n W_n(s) \exp(a_n + b_n s^{c_n}) \\ + d \cdot s]\} / \sum f^2(s) \quad (12)$$

$$\varrho_0 = \varrho_0' (\sum_{uc} f_{(s=0)}^2) / \sum_{nc} f_{(s=0)}^2 \quad (13)$$

$$I(s) = I(s) \text{ measured} / K \quad (14)$$

where K places the intensity on an absolute scale, sd refers to the shortest distances, α is an artificial damping factor that may be given a small value, if necessary to remove residual termination effects. $\varrho'(r)$ corresponds to $\varrho(r)$ minus the contributions from the shortest distances which have been removed from $i(s)$, and A scales I_b without altering its shape.

D. Least-squares refinement of RDF

The formulation of the least-squares calculation is:

$$\text{minimize } \left\{ \sum_{p < r < q} [r D'(r) + \varrho_0]^2 + w \sum_{u < r < v} [r D'(r)]^2 \right\}, \quad (15)$$

where p and q delineate the inner region, u and v delineate the outer region of the RDF and w fixes the relative weights of the two regions. It is seen from equations (10)–(14) that $D'(r)$ is defined in terms of the parameters which are to be optimized by the use of equation (15). The first sum expresses the condition that the inner region of the RDF, including that portion from which the first few distances are removed, should equal $-\varrho_0$; *i.e.*, $\varrho'(r) = 0$. The second sum expresses the condition that the outer region display a uniform distribution of distances; $\varrho'(r) = \varrho_0$. The parameters obtained from minimizing the first sum alone have been found to correspond quite closely to the parameters obtained from simultaneously varying both sums. For this reason, it is generally more economical to minimize only the first sum, *i.e.* $w = 0$, while monitoring both regions of the RDF to ensure correct behavior. Such a procedure for at least the first cycle of refinement facilitates the estimate of the lower limit of u . Optimal values for the a , b , c and A defining I_b and for K , r_{ij} , l_{ij} , ϱ_0 and N_{ij} are obtained. It was found for SiO_2 that it was necessary to remove the first three peaks, which are comprised of Si–O, O–O, and Si–Si distances, in order to rid the integral in equation (4) of

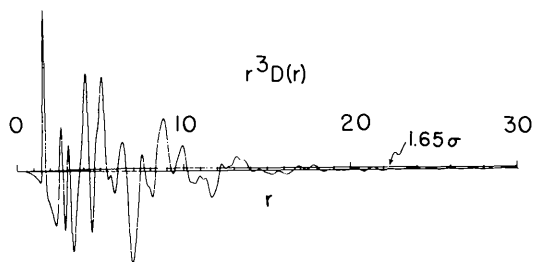


Fig. 3. The final $r^3 D(r)$ function with the first three peaks reintroduced without associated termination effects.

termination errors. It is apparent that if the N_{ij} is known for a peak that is isolated in the RDF, then fixing this value in the refinement is a sufficient constraint to obtain K and ϱ_0 . Since ϱ_0 is generally a known quantity, an independent check is provided for the scale factor. Alternatively, it is possible to fix ϱ_0 at its known value to obtain K and the N_{ij} . For the refinement of the silica-glass data, the values of the N_{ij} for three shortest distances, the Si-O, the O-O, and the Si-Si, were held constant at 8, 12, and 4 respectively.

The sequence of the refinement of the silica-glass data is outlined below. Fig. 1 shows the X-ray intensities. Table 1 indicates the parameter values and Fig. 2 illustrates the RDF at each stage of refinement. The value of α was taken as zero in the refinement; however, $\alpha = 0.0001 \cdot r^2$ for computing the RDF's in Fig. 2. Table 2 gives the total and interference intensities and Table 3 gives the radial distribution function.

The variation of α with respect to r was introduced in order to diminish the effect of the random errors at larger s on the small features of the RDF at large r .

Cycle 1.

The parameters refined were K , A , and the r_{ij} 's and l_{ij} 's for the first three distances. Detail in the inner region of the RDF was minimized from $r = 1.4$ to $r = 3.0$ Å in increments of 0.1 Å. In this region detail is due primarily to real-distance contributions and termination-error contributions. The termination error arises from a discontinuity in $si(s)$ at the experimental limit of data collection. This discontinuity is the result of real-distance contributions and, or, error in I_b at the termination point, s_{\max} . The latter possibility is the reason A is varied in this cycle. Variation of A allows errors in I_b to be limited primarily to broad features, the transform of which introduces errors into the RDF that are concentrated at $r < 1.4$ Å.

Cycle 2.

Parameters a and b were refined for each exponential function. The values for the constants c are obtained from a three-point fit of the background line in each Δs range represented by end points and the midpoint. The RDF was sampled at increments of 0.02 in the range $r = 0.02$ –3.00. The relatively small sampling increment

is necessary since the primary effects of the incorrect background are concentrated at very small r values.

Cycle 3.

The same parameters are varied as in Cycle 1.

Cycle 4.

The same parameters are varied as in Cycle 2.

The fact that $si(s) \approx 0$ at s_{\max} is a coincidence for this data set and is not a necessary condition for the refinement. The refinement proceeds in an essentially identical fashion when $s = 15$ or 15.5 is set as the limit of data instead of the true experimental value of $s = 16$.

Assessment of errors in RDF

As stated, the effect of random errors in the intensity data on the RDF may be readily estimated. Fig. 2 displays the curve representing the 1.65σ values as calculated from equation (6). There is a 10% chance that an error generated from the random errors in the intensity function will exceed the value of this curve. Since the data for silica glass are the average of 15 data sets, it is possible to calculate RDF's from different subsets of data. Reference to these RDF's and the 1.65σ error curve indicated that the main features in the final RDF out to about 20 Å are significant with

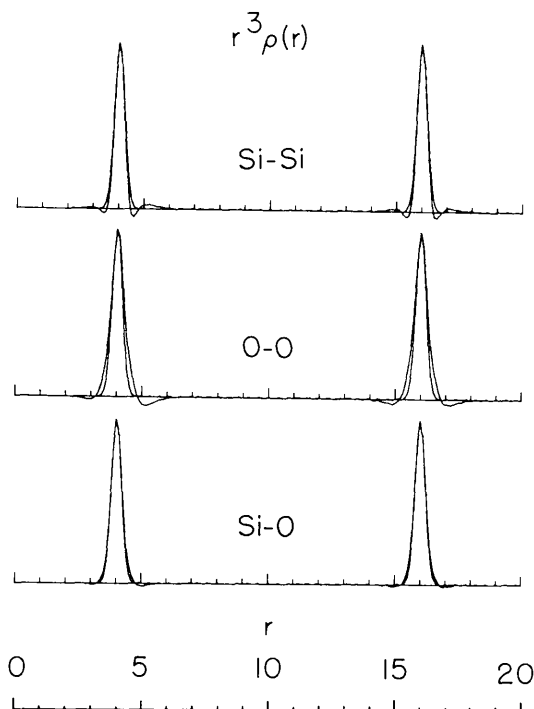


Fig. 4. RDF curves calculated with both constant and variable, neutral atom, scattering factors, $f_i f_j / \sum f^2$, for the three different types of distances. The curves are calculated with $0 \leq s \leq 16$ and $l_{ij} = 0.2$ Å.

respect to the random error of these data in agreement with the implications of Fig. 2.

The appearance of the RDF at small r , where no detail should be present may be used to evaluate the effectiveness of the termination correction (Fig. 3). It is evident from Fig. 2 that the detail disappears in successive cycles. The termination correction is further evidenced by the behavior of $si'(s)$ as illustrated in Fig 2; the function approaches zero in a smoothly oscillating fashion as s_{\max} is approached. The absence of detail with long-range periodicity at large r indicates the adequacy of the extrapolation from zero scattering angle to $s=0.3$.

The corrections for the silica glass were carried out using the ideal coordination numbers for the first three distances, as mentioned above. Alternatively, we may fix the density parameter at its measured value, 2.20 g cm^{-3} , and proceed with the data reduction treating the coordination numbers as unknown. When this is done, the radial distribution function again ultimately satisfies the imposed mathematical and physical constraints. The coordination numbers are found to be 7.99 (0.01), 11.87 (0.05), 4.13 (0.11), the distance parameters, 1.595, 2.629, 3.077 Å, and the disorder parameters, 0.0512, 0.0989, 0.1113 Å, for the smallest Si-O, O-O and Si-Si distances respectively. The numbers in the parentheses represent least-squares standard deviations and do not include contributions from systematic errors. The resulting RDF is essentially indistinguishable from the one obtained from the refinement using the ideal coordination numbers.

The function, $f_i f_j / \sum f^2$ varies slightly as a function of s . The magnitude of the errors introduced in this way may be estimated by comparing an RDF calculated with the variable scattering factors with an RDF calculated from constant scattering factors obtained as average values over the range of data collection. Representative calculations are presented in Fig. 4. The relative magnitudes of the spurious 'wings' will vary somewhat with the α value employed. The main feature to be pointed out for the purposes of this paper is that variable scattering factors may result in small errors associated with and adjacent to the main peaks in the RDF. Such spurious details related to the identifiable short distances are removed in the analysis. In regions of the RDF where a complete analysis of the peaks is not possible, though, one must exercise care in evaluating the significance of small features adjacent to the large ones. As illustrated by Fig. 4, though, the main features of the RDF are very little in error owing to the slightly variable scattering factors.

Errors in the RDF arising from scattering factors for isolated atoms that ignore bonding effects are quite small. This may be shown approximately by employing different types of scattering factors in the data reduction and observing the effects on the RDF. The RDF calculated assuming Si^{2+} and O^- is essentially the same as that obtained from neutral atoms, and the ρ_0 is found to be $0.02180 \text{ uc}/\text{\AA}^3$ instead of $0.02192 \text{ uc}/\text{\AA}^3$

which is obtained from neutral-atom scattering factors. The measured value is $0.02205 \text{ uc}/\text{\AA}^3$.

The possibility of systematic errors in the data introducing spurious details into the RDF was investigated in several ways. Tests were made with different systems for collimation and with different data collection intervals to ensure that the resolution of the intensity curve was sufficient to prevent loss of detail in the RDF. Samples of varying size were used to check for incorrect absorption corrections or detector response. A variety of samples from different sources were also used. Different diffractometers were used to further check for systematic errors. No significant effects were found.

Concluding remarks

It has been demonstrated that, by expressing the RDF explicitly as a function of parameters defining the short highly ordered distances and parameters determining the background intensity, it is possible to obtain, with a rapidly converging least-squares technique, an RDF free from termination and background errors. As illustrated in Fig. 2, the RDF changes very little after the first cycle of refinement, the cycle that removes the majority of the termination error. The second cycle shapes the background intensity quite accurately. The final two cycles are carried out to improve the values obtained for the scale factor and the parameters representing the short distances and background intensity.

It is worth noting that, if one is primarily interested in an estimate of the type and degree of long-range ordering present, but not in precise values for a scale factor and short distances, it is necessary only to collect accurate data, introduce a smooth approximate I_b , and employ a large value for α in taking the Fourier sine transform. The simpler procedure yields essentially the same RDF at large r , but with an increased breadth of the peaks which is quite evident at small r and with detail at very small r due to an incorrect I_b .

It appears that diffraction data from glasses contain structural information that has not yet been fully utilized in testing hypothesized models for glass structures. Efficient methods for obtaining this structural information should contribute much towards elucidating the atomic arrangements in glassy material.

This research was supported in part by the Advanced Research Projects Agency.

References

- CROMER, D. T. & MANN, J. B. (1968). *Acta Cryst.* **A24**, 321-324.
- D'ANTONIO, P., GEORGE, C., LOWREY, A. H. & KARLE, J. (1971). *J. Chem. Phys.* **55**, 1071-1075.
- DEBYE, P. (1915). *Ann. Phys.* **46**, 809-823.
- GUINIER, A. (1963). *X-ray Diffraction*. San Francisco: W. H. Freeman.

- KAPLOW, R., STRONG, S. L. & AVERBACH, B. L. (1965). *Phys. Rev.* **138A**, 1336–1345.
- KARLE, I. L. & KARLE, J. (1949). *J. Chem. Phys.* **17**, 1052–1058;
- KARLE, I. L. & KARLE, J. (1950). *J. Chem. Phys.* **18**, 957–962, 963–971.
- KONNERT, J. H. & KARLE, J. (1972). *Nature Phys. Sci.* **236**, 92–94.
- KONNERT, J. H., KARLE, J. & FERGUSON, G. A. (1973). *Science*, **179**, 177–179.
- LEADBETTER, A. J. & WRIGHT, A. C. (1972). *J. Non-Cryst. Solids*, **7**, 141–155.
- WARREN, B. E. (1969). *X-ray Diffraction*. Reading, Mass. Addison-Wesley.
- ZERNICKE, F. & PRINS, J. A. (1927). *Z. Phys.* **41**, 184–194.

Acta Cryst. (1973). **A29**, 710

Periodicity in Thickness of Electron-Microscope Crystal-Lattice Images

BY P. L. FEJES, SUMIO IJIMA AND J. M. COWLEY

Department of Physics, Arizona State University, Tempe, Arizona, 85281, U.S.A.

(Received 24 April 1973; accepted 12 June 1973)

High-resolution electron micrographs of crystal lattices showing a recognizable correlation of intensity with atom positions are normally obtained only for very thin crystals (less than about 100 Å thick). For some crystals of niobium and titanium–niobium oxides, it has been observed that this thin-crystal contrast is repeated for thicknesses of the order of 1000 Å. This is regarded as evidence that under conditions of high symmetry of excitation, the wave field in the crystal is essentially periodic with distance in the beam direction if a particular relationship exists between the structure amplitudes and the excitation errors for the diffraction process. This is confirmed by calculations made for f.c.c. lattices with Cu, CuAu₃, or Au atoms and for a range of wavelengths.

Introduction

It has been shown recently (Iijima, 1971) that, when a thin crystal is aligned so that the incident electron beam is parallel to a principal axis, high-resolution electron micrographs can be obtained which show a direct correlation between image intensity and the projection of the crystal structure. In this way the distribution of metal atoms in a number of oxide phases has been determined both for perfect crystal regions and for linear or planar faults in the structures (Iijima, 1972, 1973; Iijima & Allpress, 1973). The nature of the contrast observed can be understood semi-quantitatively by application of the phase-object approximation (Cowley & Iijima, 1972). It is observed that when the crystal thickness exceeds that for which the phase-object approximation is expected to be valid, namely about 100 Å for 100 keV electrons, the image contrast no longer shows any obvious relationship to the crystal structure. This may be associated with the onset of three-dimensional dynamical diffraction conditions under which the variations of the relative phases and amplitudes of the many diffracted waves are very complicated and, in general, show no apparent periodicity with increasing thickness. However, for a few special cases an almost exact repetition of the thin-crystal contrast has been observed for relatively large thicknesses suggesting a recurrence of very nearly the same relative amplitudes and phases of the diffracted beams.

Observations

Fig. 1 is part of an electron micrograph of a crystal of the high-temperature phase, *H*-Nb₂O₅. The incident beam is parallel (within 3×10^{-3} radians) to the short *b* axis ($b = 3.8$ Å) of the monoclinic unit cell ($a = 21.2$, $c = 19.4$ Å, $\beta = 120^\circ$) and the image is obtained with approximately the 'optimum defocus' for phase contrast, $\Delta f = -900$ Å, using a modified JEM-100B electron microscope with a goniometer stage. Thickness determinations of the crystal were made by the observation of the images of planar faults for various tilts of the crystal. The crystal is wedge-shaped with an almost linear increase in thickness.

In the thin part of the crystal, near the edge of the wedge, the lattice image clearly shows the configuration of metal atoms within the unit cell which includes 4×3 and 5×3 blocks of ReO₃-type corner-sharing octahedra, plus atoms in tetrahedral positions which generate the darkest spots. A detailed study of the lattice images of *H*-Nb₂O₅ in both ordered and disordered forms has been reported by Iijima (1973) (see also Anderson, Browne & Hutchinson, 1972). With increasing crystal thickness this readily interpreted form of the image is lost for thicknesses of 100–150 Å and is replaced by a variety of image forms, none of which has any obvious relationship to the structure. Then for thicknesses of about 500 to 800 Å the thin-crystal image reappears with much the same contrast as for